JACC: BASIC TO TRANSLATIONAL SCIENCE VOL. 9, NO. 9, 2024

ORIGINAL RESEARCH - PRECLINICAL

TRIM55 Aggravates Cardiomyocyte Apoptosis After Myocardial Infarction via Modulation of the Nrf2/HO-1 Pathway

Yuxin Bu, MM,* Yanxia Liu, MD,* Meili Liu, MD, Chenghui Yan, MD, Jing Wang, MM, Hanlin Wu, MM, Haixu Song, MD, Dali Zhang, MD, Kai Xu, MD, Dan Liu, MD, Yaling Han, MD, PhD

VISUAL ABSTRACT

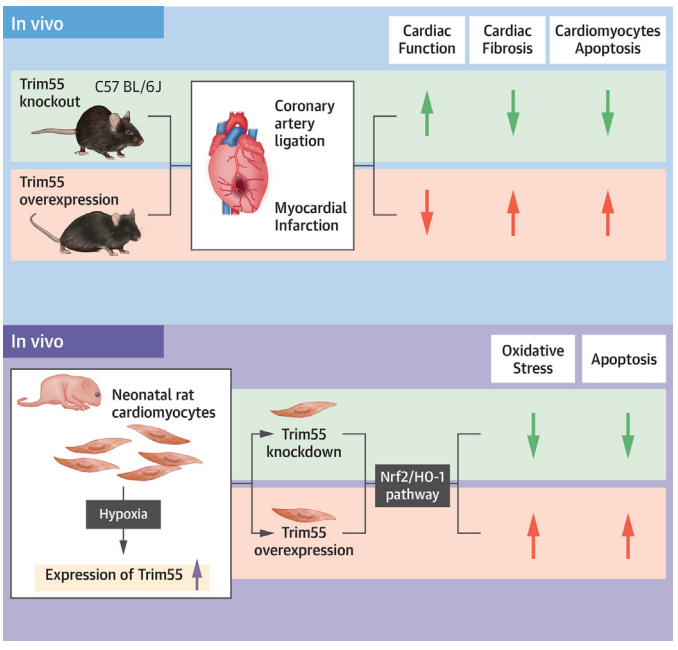

Bu Y, et al. JACC Basic Transl Sci. 2024;9(9):1104–1122.

HIGHLIGHTS

- **Trim55 knockout improved cardiac dysfunction and cardiomyocyte apoptosis after MI, whereas overexpression aggravated cardiac dysfunction after MI.**
- **Trim55 regulated cardiomyocyte apoptosis by inhibiting the Nrf2/HO-1 pathway.**
- **Trim55 regulated the Nrf2/HO-1 pathway by interacting with Nrf2.**
- **Trim55 was regulated by the transcription factor Foxo3 under hypoxia.**

From the State Key Laboratory of Frigid Zone Cardiovascular Diseases, Cardiovascular Research Institute and Department of Cardiology, General Hospital of Northern Theater Command, Shenyang, China. *Drs Bu and Y. Liu contributed equally to this work and are joint first authors.

The authors attest they are in compliance with human studies committees and animal welfare regulations of the authors' institutions and Food and Drug Administration guidelines, including patient consent where appropriate. For more information, visit the Author Center.

Manuscript received September 27, 2023; revised manuscript received May 24, 2024, accepted May 24, 2024.

ISSN 2452-302X https://doi.org/10.1016/j.jacbts.2024.05.006

SUMMARY

Tripartite motif-containing 55 (Trim55) is mainly expressed in myocardium and skeletal muscle, which plays an important role in promoting the embryonic development of the mouse heart. We investigated the role of Trim55 in myocardial infarction and the associated molecular mechanisms. We studied both gain and loss of function in vivo and in vitro. The results showed that Trim55 knockout improved cardiac function and apoptosis after myocardial infarction, and overexpression aggravated cardiac function damage. The mechanism is that Trim55 interacts with nuclear factor, erythroid derived 2 (Nrf2) to accelerate its degradation and inhibit the expression of heme oxygenase 1, thereby promoting cardiomyocyte apoptosis. (JACC Basic Transl Sci. 2024;9:1104–1122)

Myocardial infarction (MI) is a major public health problem with a high global prevalence and mortality rate.[1,2] MI-related heart failure remains a major problem without targeted therapy. Many factors, such as loss of cardiomyocytes, inflammation, and myocardial fibrosis, are associated with MI progression. Cardiomyocyte loss is the primary cause of MI-induced cardiac injury and dysfunction caused by MI.[3] Cardiomyocyte apoptosis is an important cause of cardiomyocyte loss after MI and promotes the progression of myocardial fibrosis and heart failure after MI.[4] Nevertheless, no therapeutic intervention targeting cardiomyocyte apoptosis has been clinically proven to be effective for treating MI. Therefore, identifying a key method for preventing cardiomyocyte apoptosis after MI could provide new strategies for preventing and treating MI.

Tripartite motif-containing 55 (Trim55), an E3 ubiquitin ligase highly expressed in the myocardium and skeletal muscles, plays an important role in skeletal muscle differentiation and myofibrillogenesis.[5,6] Trim55 plays critical roles in nonmuscle tissues and cells. For example, Trim55 can rescue lipopolysaccharide (LPS)-induced hepatitis by inhibiting nuclear factor kappa B production and macrophage migration[7]; Trim55 is an independent factor affecting the prognosis of patients with hepatocellular carcinoma, and Trim55 overexpression inhibits migration and invasion of hepatocellular carcinoma cells.[8] Recently, Trim55 has been reported to play important roles in cardiovascular diseases. Trim55 is a novel candidate gene for left ventricular hypertrophy independent of blood pressure.[9] The rare variants of Trim55 are related to the severity of human hypertrophic cardiomyopathy.[10] Trim55 gene knockout aggravates diabetic cardiomyopathy by regulating cardiac peroxisome proliferator-activated receptor (PPAR) α1 and PPARγ1 activities via post-translational modification.[11] Alternatively, Tan et al[12] showed that Trim55, as a downstream target of miR-378a-5p, protects the heart from ischemia-reperfusion injury by reducing c-Jun NH2-terminal kinase 1/2 (JNK1/2) activation. However, whether Trim55 also promotes cardiomyocyte apoptosis during persistent ischemia post-MI and whether altered Trim55 gene expression plays important roles in cardiomyocyte apoptosis post-MI remain unclear.

In this study, we investigated the roles and mechanisms of Trim55 in MI through gain-of-function and loss-of-function in vivo and in vitro. We observed that Trim55 knockout reduced cardiomyocyte apoptosis and myocardial fibrosis after MI. At the same time, Trim55 overexpression increased cardiomyocyte apoptosis and myocardial fibrosis after MI. Our results suggest that Trim55 could be a potential therapeutic target for MI treatment in clinical trials.

ABBREVIATIONS AND ACRONYMS

AAV = adeno-associated virus
Bax = BCL2 associated X apoptosis regulator
Bcl-2 = BCL2 apoptosis regulator
CHX = cycloheximide
$CoCl_2$ = cobalt chloride
CQ = chloroquine
DMEM = Dulbecco's modified Eagle medium
FBS = fetal bovine serum
Foxo3 = forkhead box transcription factor 3
HO = heme oxygenase
LPS = lipopolysaccharide
MG132 = N-Cbz-Leu-Leu-leucinal
MI = myocardial infarction
mRNA = messenger RNA
NRCM = neonatal rat cardiomyocyte
Nrf2 = nuclear factor, erythroid derived 2
PBS = phosphate-buffered saline
PCR = polymerase chain reaction
PPAR = peroxisome proliferator-activated receptor
ROS = reactive oxygen species
siRNA = small interfering RNA
Trim55 = tripartite motif-containing 55
TUNEL = terminal deoxynucleotidyl transferase-mediated dUTP nick end labeling
WT = wild type

METHODS

ANIMALS. Adult C57BL/6J mice (8-10 weeks old; weight: 21-23 g; male) were purchased from Gem-Pharmatech Co, Ltd. The mice were maintained at 23 °C ± 3 °C and 30% to 70% humidity, with 12 hours of light/12 hours of dark circulation, and could freely obtain food and water. Animal care was approved by the Ethics Committee on the Ca-re and Use of Laboratory Animals of the General Hospital of the Northern Theater Command.

Trim55-knockout mice ($Trim55^{-/-}$) with a C57BL/6J (wild type [WT]) background were generated. Male $Trim55^{-/-}$ mice aged 8 to 10 weeks and littermate

control C57 mice were randomly divided into 4 groups: C57-sham (n = 10), C57-MI (n = 20), $Trim55^{-/-}$-sham (n = 10), and $Trim55^{-/-}$-MI (n = 20). To generate Trim55-overexpressing mice, adeno-associated virus (AAV) overexpressing Trim55 (AAV2/9-CMV-Trim55, 2×10^{11} genome copies per mouse in 200 μL of saline [OBiO Technology]) was injected into C57 mice by tail vein injection. After 3 weeks, the mice were randomly divided into 4 groups: AAV-CON-sham (n = 8), AAV-CON-MI (n = 15), AAV-Trim55-sham (n = 8), and AAV-Trim55-MI (n = 17). Randomization and blinding were performed. No mice were excluded from the study unless they died.

MI MODEL ESTABLISHMENT. The MI model was established using the internationally recognized technique of permanent coronary artery ligation (left anterior descending coronary artery).[13] First, mice were anesthetized with 2% isoflurane inhalation. Ophthalmic scissors were used to gently cut the skin between the third and fourth ribs of the left chest. After blunt separation of the small opening in the pleura, the left and right hands worked together to quickly squeeze the heart and locate the left anterior descending branch of the coronary artery. Approximately 2 mm from the lower edge of the left atrial appendage, the left anterior descending branch was quickly ligated using a 6-0 needle suture, and the apex of the heart turned white. The ultrasound-connected electrocardiogram of the small animal showed a typical manifestation of MI, indicating successful ligation.

SURVIVAL ANALYSIS. Four weeks after establishing the MI model, the cumulative mortality of control mice, Trim55-overexpressing mice, and Trim55-knockout mice was calculated. Kaplan-Meier survival curves were compared by log-rank test using GraphPad Prism version 8.0.2 for Windows (GraphPad Software).

ECHOCARDIOGRAPHIC MEASUREMENTS. Transthoracic echocardiography was performed to evaluate cardiac function in mice via a Vevo2100 High-Resolution Imaging System (FUJIFILM Visual Sonics) equipped with a 10-MHz phased-array transducer with M-mode recording. Briefly, mice were anesthetized with 2% isoflurane inhalation. Two-dimensional targeted M-mode traces were recorded from the parasternal short-axis view at the midpapillary muscle level and the parasternal long-axis view at the level immediately under the papillary muscle. The left ventricular parameters, including left ventricular diastolic anterior wall thickness, left ventricular systolic anterior wall thickness, left ventricular internal dimension at end diastole, and left ventricular internal dimension at systole, were measured based on M-mode recordings. The data were represented as the average of measurements of 3 consecutive beats. Mice were anesthetized by inhalation of isoflurane mixed with pure oxygen at a concentration of 2% to 3% for induction of anesthesia and 1.5% to 2% for maintenance of anesthesia. Mice were sacrificed by cervical dislocation, and the hearts were quickly removed and placed in liquid nitrogen or 4% paraformaldehyde for subsequent experiments.

CELL CULTURE AND TREATMENT. Neonatal rat ventricular cells (neonatal rat cardiomyocytes [NRCMs]) were isolated and cultured using previously reported procedures.[14] Briefly, after rinsing in phosphate-buffered saline (PBS), the isolated hearts of neonatal rats were cut into pieces and digested with 0.25% trypsin. The obtained NRCMs were cultured in Dulbecco's modified Eagle medium (DMEM) (HyClone Laboratories) supplemented with 10% fetal bovine serum (FBS) (Gibco), 100 U/mL penicillin, and 100 g/mL streptomycin. NRCMs were grown at 37 °C in a humid atmosphere of 5% CO_2 and 95% air. After 48 hours, the cells were transfected with the relevant plasmids, small interfering RNAs (siRNAs), and vectors.

The H9C2 cells were purchased from FuHeng Cell Center (FH-1004). H9C2 cells were seeded in 6-well plates at a density of 2×10^5 cells/well and cultured with DMEM supplemented with 10% FBS in a humid atmosphere of 5% CO_2 and 95% air.

To simulate hypoxic conditions, cobalt chloride ($CoCl_2$) was used in our study. $CoCl_2$ was obtained from the Sigma-Aldrich (7791-13-1) and dissolved in deionized water to make a 100-mmol/L stock solution, filtered before use. The NRCMs were treated with $CoCl_2$ for different concentrations (0, 200, 400, 600, and 800 μmol/L) or treated with $CoCl_2$ for different time periods (0, 6, 12, 24, and 48 hours). To investigate the mechanism of Trim55 on cell apoptosis after hypoxia, NRCMs or H9C2 cells were treated with or without 400 μmol/L $CoCl_2$ for 24 hours and then cultured in DMEM with 10% FBS at 37 °C in 5% CO_2.

ADENOVIRUS, PLASMID, AND siRNA TRANSFECTION. To establish Trim55-overexpressing or -knockdown cells, NRCMs were transfected with Trim55-overexpressing adenovirus (adTrim55, OBiO Technology) or Trim55-interfering RNA (si-Trim55, RiboBio). To establish cells with forkhead box transcription factor 3 (Foxo3); nuclear factor, erythroid derived 2 (Nrf2); or heme oxygenase 1 (HO-1) overexpression or knockdown, NRCMs were transfected with Foxo3-overexpressed plasmid (pcDNA3.1-Foxo3, GENEWIZ), Nrf2-

overexpressed plasmid (pcDNA3.1-6xHis-Nrf2, GENEWIZ), HO-1-overexpressed plasmid (pcDNA3.1-HO-1, GENEWIZ), siRNA-targeting Nrf2 (si-Nrf2, Santa Cruz Biotechnology), siRNA-targeting Foxo3 (si-Foxo3, RiboBio), or siRNA-targeting HO-1 (si-HO-1, RiboBio) using Lipofectamine 2000 (Invitrogen), respectively.

HISTOMORPHOLOGIC ANALYSIS. Mice were anesthetized by inhalation of isoflurane mixed with pure oxygen at a concentration of 2% to 3% for induction of anesthesia and 1.5% to 2% for maintenance of anesthesia. Mice were sacrificed by cervical dislocation at 3 and 28 days after MI, and the hearts were harvested and fixed overnight in 4% paraformaldehyde and embedded in paraffin according to standard organizational procedures. Each heart was cut into 5 pieces of 4- to 5-μm-thick serial sections. Hematoxylin and eosin staining was used to explore the changes in heart size, and Masson's trichrome staining (Solarbio) was performed to analyze the fibrosis area of MI.

IMMUNOHISTOCHEMICAL STAINING. Immunohistochemical staining was performed according to the manufacturer's instructions (KIT9709, MX Biotechnology). After rehydration in citrate buffer solution and a 40-minute antigen recovery process, mouse heart slices were permeabilized with 0.2% Triton X-100 in PBS for 15 minutes, sealed with 5% bovine serum albumin for 1 hour, and stained overnight with Trim55 (1:50, Thermo Fisher Scientific) antibody. After washing 3 times in PBS, all samples were dyed, dehydrated, made transparent with diaminobenzidine and hematoxylin, and finally sealed with a cover glass and neutral gum. A microscope (Zeiss) was used to capture histologic changes. ImageJ (National Institutes of Health) software was used to estimate the expression level of Trim55.

TERMINAL DEOXYNUCLEOTIDYL TRANSFERASE-MEDIATED dUTP NICK END LABELING ASSAY. To evaluate cell apoptosis, cell slides and fresh frozen heart sections were labeled using an in situ cell death detection kit (Roche) according to the manufacturer's instructions. After terminal deoxynucleotidyl transferase-mediated dUTP nick end labeling (TUNEL) staining, nuclei were stained with 4′,6-diamidino-2-phenylindole (Biosharp). TUNEL-positive cells were observed under a fluorescence microscope (Zeiss), and the ratio of TUNEL-positive cells to 4′,6-diamidino-2-phenylindole-positive nuclei was calculated.

WESTERN BLOT. Total protein was extracted from cardiomyocytes or myocardium with radioimmunoprecipitation assay lysis buffer (Thermo Fisher Scientific). Protein concentration was determined by using the BCA protein assay kit (Thermo Fisher Scientific). Protein lysates were separated by 8%, 10%, and 15% (volume/volume) sodium dodecyl sulfate polyacrylamide gels and then transferred onto nitrocellulose membrane (Millipore) for subsequent studies. After blocking with 5% nonfat milk at room temperature for 2 hours, the membrane was incubated with the primary antibody at 4 °C for overnight. Then, the secondary antibody was used to conjugate the membrane at room temperature for 1 to 2 hours. The primary antibodies were used as follows: glyceraldehyde-3-phosphate dehydrogenase antibody (2118S, Cell Signaling Technology), Trim55 antibody (A15917, Abclonal), BCL2-associated X apoptosis regulator (Bax) antibody (2772S, Cell Signaling Technology), BCL2 apoptosis regulator (Bcl2) antibody (ab182858, Abcam), cleaved caspase-3 antibody (9664S, Cell Signaling Technology), cleaved caspase-8 antibody (8592S, Cell Signaling Technology), transforming growth factor-β antibody (3709S, Cell Signaling Technology), collagen I antibody (ab270993, Abcam), HO-1 antibody (ab189491, Abcam), Nrf2 antibody (A0674, Abclonal), and Foxo3 antibody (A9270, Abclonal).

REAL-TIME POLYMERASE CHAIN REACTION. Total RNA was extracted from cardiomyocytes or myocardium using TRIzol reagent (15596018CN, Thermo Fisher Scientific). Total RNA was subjected to reverse transcription reactions using the Takara reverse transcription kit, followed by real-time quantitative polymerase chain reaction (PCR) using a BIO-RAD PCR system (CFX96). Real-time PCR amplification was performed as follows: 95 °C for 5 minutes and 40 cycles at 95 °C for 20 seconds, 55 °C for 20 seconds, and 72 °C for 20 seconds; 18S ribosomal RNA was used as an internal control. The relative quantitative expression was determined using the $2^{-\Delta\Delta CT}$ method. The primer pairs were synthesized by Sangon, as described in Supplemental Table 1.

DETECTION OF REACTIVE OXYGEN SPECIES CONTENT. The intracellular reactive oxygen species (ROS) content was measured by CellROX staining.[15] (C10491, Thermo). The cultured cells were washed with PBS and incubated with 10 μmol/L fluorescent dyes at 37 °C for 30 minutes according to the manufacturer's instructions. The cells were washed 3 times with PBS and stained at 20 to 25 °C with 2.5 μmol/L Hoechst 33342 (HY-15559, MCE) for 5 minutes. Fluorescence intensity was obtained by confocal fluorescence microscopy (LSM 900, Zeiss) and the BD FACS Aria system (BD Pharmingen). The data were analyzed by Image-Pro Plus software (Media Cybernetics) and FlowJo software (Stanford University Leonard

Herzenberg Laboratory). The results were obtained from 3 independent experiments.

APOPTOSIS DETECTION BY FLOW CYTOMETRY. The percentage of apoptotic cells was assessed through flow cytometry using an annexin V-PE/7-aminoactinomycin D apoptosis detection kit (catalog no. 559763, BD Pharmingen) as previously described.[16] The culture media and adherent NRCMs were collected after the corresponding treatments. The precipitate was washed with precooled PBS, resuspended in 1× binding buffer, and incubated with annexin V-PE and annexin V-PE/7-aminoactinomycin D dye solutions for 15 minutes at room temperature in the dark. Finally, the samples were tested using the BD FACS Aria system (BD Pharmingen), and the data were analyzed using FlowJo software.

PROTEIN HALF-LIFE AND DEGRADATION PATHWAY DETECTION. The half-life of Nrf2 in cardiomyocytes was measured by protein synthesis inhibitor cycloheximide (CHX) (HY-12320, MCE). CHX dissolved in dimethyl sulfoxide and was added to cells at a final concentration of 100 ng/mL. Proteasome inhibitor N-Cbz-Leu-Leu-leucinal (MG132) (HY-13259, MCE) and autophagy inhibitor chloroquine (CQ) (HY-17589A, MCE) were used to detect the degradation pathway of Nrf2 in cardiomyocytes. MG132 or CQ was dissolved in dimethyl sulfoxide and was added to cells at a final concentration of 10 μmol/L.

JASPAR DATABASE ANALYSIS. The JASPAR database (https://jaspar.genereg.net/) was used to identify transcription factor binding sites in the eukaryotic genome. This database was used to identify the upstream transcription factor of Trim55 gene.

DUAL-LUCIFERASE REPORTER ASSAY. HEK293T cells were seeded in a 24-well plate and transfected with or without firefly luciferase reporter plasmids encoding the Trim55 promoter (WT-Trim55), the Trim55 promoter with a binding site mutant (Mut-Trim55), and Foxo3 luciferase reporter plasmids. After 24 hours of transfection, the cells were collected, washed twice with PBS, and then lysed with 100 μL passive lysis buffer for 15 minutes at 37 °C. Luciferase activity was measured using the Dual-Luciferase Reporter Assay System on a SpectraMax i3X Multi-Mode Microplate Reader (Molecular Devices). Luciferase activity was defined as the ratio of firefly luciferase activity to *Renilla* luciferase activity, and the luciferase activity of the empty vector (pGL3-Basic) was set to 1.

STATISTICAL ANALYSIS. Kaplan-Meier methods (log-rank test) were used to estimate and compare survival curves. The Pearson correlation coefficient (r) was used to evaluate the relationship between 2 continuous variables. Student's t-test was used to detect differences between groups. Single-factor or 2-way analysis of variance with the Bonferroni post hoc test for multiple pairwise comparisons was used to compare multiple groups. A P value of <0.05 is defined as statistically significant. All data are represented as mean ± SEM and were analyzed using GraphPad Prism version 8.0.2 for Windows.[17]

RESULTS

TRIM55 EXPRESSION WAS UPREGULATED IN THE BORDER ZONE OF MI HEARTS AND HYPOXIC CARDIOMYOCYTES. Initially, a mouse MI model was established and assessed by using the cardiac function and histologic morphology at different timepoints. The findings indicated that the MI model was effectively established (Supplemental Figures 1A to 1E).

To evaluate the role of Trim55 in myocardial injury after MI, we first examined the Trim55 expression under hypoxic conditions in vivo and in vitro. Compared with that in the sham group, the messenger RNA (mRNA) and protein levels of Trim55 were significantly increased in the infarct border zone of myocardium of the MI group (**Figures 1A to 1C**). Immunohistochemical staining showed that the expression of Trim55 was also significantly increased in the myocardium after MI (**Figures 1D and 1E**). In vitro, $CoCl_2$ was used to induce hypoxia in cardiomyocytes[18] and significantly increased the expression of hypoxia-inducible factor 1α (HIF1α) in NRCMs (Supplemental Figures 2A and 2B). $CoCl_2$ increased the mRNA and protein expression of Trim55 in a time- and concentration-dependent manner. Therefore, 400 μmol/L $CoCl_2$ for 24 hours was used in the following experiments (**Figures 1F to 1H**, Supplemental Figures 2C to 2H).

TRIM55 KNOCKOUT AMELIORATED CARDIAC INJURY AFTER MI. To clarify the role of Trim55 in cardiac injury after MI, we first examined the tissue expression profile of Trim55 in C57 mice and observed that Trim55 was specifically expressed in the heart and skeletal muscle (Supplemental Figure 3A). Next, we used CRISPR/Cas9 technology to generate $Trim55^{-/-}$ mice (Supplemental Figure 3B) and confirmed that Trim55 was successfully deleted in the heart by using genotyping, Western blot, and real-time PCR (Supplemental Figures 3C to 3E). We found that Trim55 deletion in the heart had no effect on cardiac function in C57 mice (Supplemental Table 2).

Furthermore, Trim55-knockout mice and their littermate C57 mice were used to establish the MI

FIGURE 1 Trim55 Expression Was Significantly Increased After MI

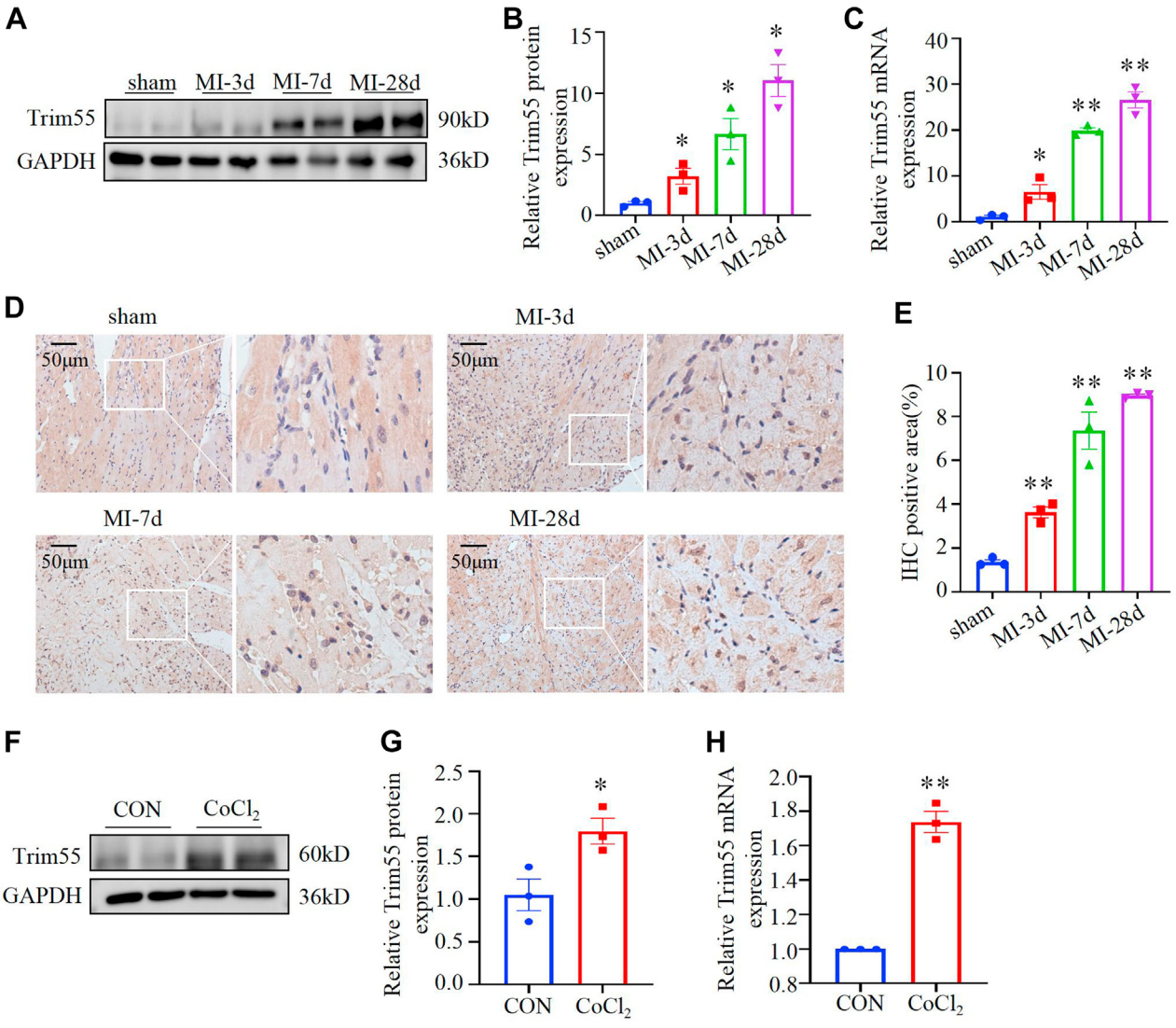

(A, B) Quantification and representative images of Western blot analyses showing Trim55 protein expression in the border zone of myocardium at 3, 7, and 28 days after MI (n = 3). (C) Quantification of Trim55 mRNA levels in the border zone of myocardium at 3, 7, and 28 days after MI (n = 3). (D, E) Quantification and representative images of Trim55 immunohistochemistry in the border zone of myocardium at 3 and 28 days after MI (n = 3; scale bar: 50 μm). (F, G) Quantification and representative images of Western blot analyses showing Trim55 protein expression in NRCM cells after 400 μmol/L stimulation at 24 hours (n = 3). (H) Quantification of Trim55 mRNA levels in NRCM cells after $CoCl_2$ stimulation (400 μmol/L; 24 hours; n = 3). All data are expressed as mean ± SEM. Data in B, C, E, G, and H were analyzed using Student's *t*-test. *$P < 0.05$, **$P < 0.01$ vs the control or sham group. $CoCl_2$ = cobalt chloride; CON = control; GADPH = glyceraldehyde-3-phosphate dehydrogenase; IHC = immunohistochemistry; MI = myocardial infarction; mRNA = messenger RNA; NRCM = neonatal rat cardiomyocyte; Trim55 = tripartite motif-containing 55.

model; the flow chart of establishing the MI model is shown in Supplemental Figure 3F. During MI, the mortality was lower in the Trim55$^{-/-}$ group than that in WT group (Supplemental Figure 3G). Compared with the C57-MI group, the Trim55$^{-/-}$-MI group showed significantly improved left ventricular ejection fraction, fractional shortening, and left ventricular chamber diameters in diastole and systole (**Figure 2A**, Supplemental Figures 3H and 3I). Additionally, the ratio of heart weight to body weight and the extent of the infarct size after MI was decreased by Trim55 gene knockout (**Figures 2B to 2D**). The hearts in the Trim55$^{-/-}$-MI group showed lower levels of collagen I and transforming growth factor β in the

FIGURE 2 Trim55 Knockout Alleviated Myocardial Injury and Cardiomyocyte Apoptosis After MI

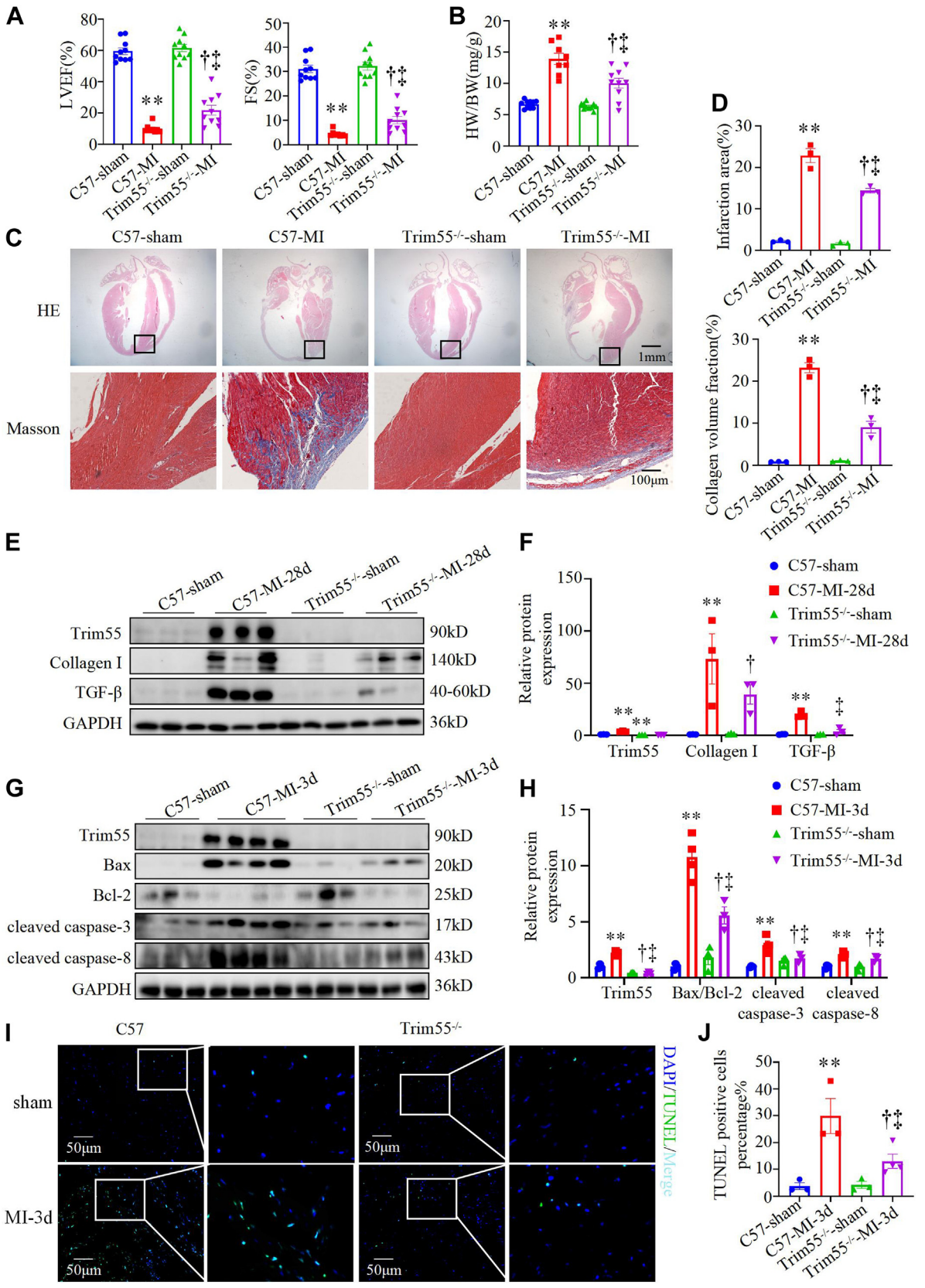

Continued on the next page

border zone of myocardium at 28 days post-MI (**Figures 2E and 2F**), suggesting that Trim55 knockout reduced the degree of cardiac fibrosis post-MI.

In addition, cardiomyocyte apoptosis was examined in the sham and MI group of C57 and Trim55$^{-/-}$ mice. Compared with the C57-MI group, the ratio of Bax/Bcl-2 and cleaved caspase-3 levels in the border zone of Trim55$^{-/-}$ hearts was decreased at 3 days post-MI. Simultaneously, TUNEL assay showed a notable decrease in apoptotic cells in the border region of Trim55$^{-/-}$ knockout hearts (**Figures 2G to 2J**). In summary, these findings indicate that Trim55 knockout alleviated cardiac injury during MI, which was related to a decrease in the apoptosis of cardiomyocytes within the border zone of myocardium.

TRIM55 OVEREXPRESSION AGGRAVATED CARDIAC INJURY AFTER MI. To further elucidate the role of Trim55 overexpression in cardiac injury following MI, we generated Trim55 whole-body-overexpressing mice (Supplemental Figures 4A and 4B), AAV control (AAV-CON) and AAV-Trim55 were injected into 8-week-old C57 mice via the tail vein, and an MI model was established at 3 weeks after virus injection (Supplemental Figure 4C). The survival rates in the control and MI groups of AAV-CON and AAV-Trim55 were evaluated at 28 days after MI, and we found that no significant difference existed between the MI group of AAV-CON and AAV-Trim55 (Supplemental Figure 4D). Compared with the AAV-CON-MI group, the left ventricular ejection fraction and fractional shortening were significantly decreased in the AAV-Trim55-MI group at 28 days post-MI (Supplemental Figures 4E, 4F, and 5A). In contrast, the ratio of heart weight to body weight was substantially increased in the AAV-Trim55-MI group (Supplemental Figure 5B).

At 28 days after MI, Trim55-overexpressing mice showed a significant increase in both infarct size and fibrosis in the border zone compared with the AAV-CON-MI group (Supplemental Figures 5C and 5D). The levels of collagen I and transforming growth factor-β in the border zone of the Trim55-overexpressing mice were increased at 28 days after MI (Supplemental Figures 5E and 5F). These results indicate that Trim55 overexpression increased the degree of cardiac fibrosis after MI.

Furthermore, the ratio of Bax/Bcl-2 and cleaved caspase-3 expression levels were significantly higher in AAV-Trim55-MI mice than in AAV-CON-MI mice (Supplemental Figures 5G and 5H). The overexpression of Trim55 increased the number of TUNEL-positive cells after MI (Supplemental Figures 5I and 5J). In summary, Trim55 overexpression exacerbated cardiac injury following MI.

TRIM55 OVEREXPRESSION AGGRAVATED CARDIOMYOCYTE APOPTOSIS INDUCED BY HYPOXIA. To further examine the effect of Trim55 on cardiomyocyte apoptosis, we used $CoCl_2$ to stimulate NRCMs in vitro. adTrim55 was infected into NRCMs to establish Trim55-overexpressing cells (**Figure 3A**), and we examined whether Trim55 overexpression could have deleterious effects on cardiomyocyte apoptosis. Compared with the adenovirus control (adcon) group, the cleaved caspase-3 and cleaved caspase-8 levels were significantly increased in adTrim55 group, whereas the endogenous apoptosis markers, including cleaved caspase-9 and Bcl-2, were not changed (**Figures 3A and 3B**).

Subsequently, hypoxia was induced by $CoCl_2$ in Trim55-overexpressing cardiomyocytes. Cardiomyocyte apoptosis was assessed using Western blot, annexin V-PE/7AAD staining, and TUNEL assay. The results revealed that overexpression of Trim55 resulted in a significant elevation in the protein levels of cleaved caspase-3 and cleaved caspase-8 and an increase in the number of apoptosis-positive cardiomyocytes following treatment with $CoCl_2$ (**Figures 3C to 3H**). These findings indicate that the upregulation of Trim55 exacerbated cardiomyocyte apoptosis triggered by hypoxia.

FIGURE 2 Continued

(A) Echocardiographic analysis of the LVEF and FS at 28 days after MI in the C57-sham (n = 10), Trim55$^{-/-}$-sham (n = 10), C57-MI (n = 10), and Trim55$^{-/-}$-MI (n = 10) groups. (B) Quantitative analysis of the ratio of heart weight to body weight at 28 days after MI in the C57-sham (n = 10), Trim55$^{-/-}$-sham (n = 10), C57-MI (n = 8), and Trim55$^{-/-}$-MI (n = 10) groups. (C, D) Representative HE and Masson staining pictures and quantification of the infarction area at 28 days after MI in the C57-sham, Trim55$^{-/-}$-sham, C57-MI, and Trim55$^{-/-}$-MI groups (n = 3). (E, F) Quantification and representative images of Western blot analyses showing the Trim55, collagen I, and TGF-β protein expression in the C57-sham, Trim55$^{-/-}$-sham, C57-MI, and Trim55$^{-/-}$-MI groups (n = 3). (G, H) Quantification and representative images of Western blot analyses showing the Trim55, Bax, Bcl2, cleaved caspase-3, and cleaved caspase-8 protein expression in the C57-sham (n = 3), Trim55$^{-/-}$-sham (n = 3), C57-MI (n = 4), and Trim55$^{-/-}$-MI (n = 3) groups. (I, J) Representative TUNEL staining images and quantification of apoptotic positive cells at 3 days after MI in the C57-sham (n = 3), Trim55$^{-/-}$-sham (n = 3), C57-MI (n = 3), and Trim55$^{-/-}$-MI (n = 4) groups. All data in A, B, D, F, H, and J are expressed as mean ± SEM. Data in A, B, D, F, H, and J were analyzed using 2-way analysis of variance followed by the Bonferroni post hoc test. $^{**}P < 0.01$ vs C57-sham; $^{\dagger}P < 0.05$ vs Trim55$^{-/-}$-sham; $^{\ddagger}P < 0.05$ vs C57-MI. Bax = BCL2 associated X apoptosis regulator; Bcl-2 = BCL2 apoptosis regulator; BW = body weight; FS = fraction shortening; HE = hematoxylin and eosin; HW = heart weight; LVEF = left ventricular ejection fraction; TGF = transforming growth factor; TUNEL = terminal deoxynucleotidyl transferase–mediated dUTP nick end labeling; other abbreviations as in **Figure 1**.

KNOCKDOWN OF TRIM55 ATTENUATED CARDIOMYOCYTE APOPTOSIS INDUCED BY HYPOXIA. To examine the effect of Trim55 knockout on cardiomyocyte apoptosis, NRCMs were infected with Trim55-interfering RNA (**Figure 4A**). The cleaved caspase-3 and cleaved caspase-8 levels were significantly reduced in Trim55-knockdown cardiomyocytes (**Figures 4A and 4B**). The levels of endogenous apoptotic markers, including cleaved caspase-9 and Bcl-2, did not exhibit significant alterations, which was similar to the observed in Trim55-overexpression group.

To prove that whether Trim55 knockdown could influence cardiomyocyte apoptosis after hypoxia, Western blot, annexin V-PE/7AAD staining, and TUNEL assay were also conducted. Trim55 knockdown reduced the protein expressions of cleaved caspase-3 and cleaved caspase-8 and the percentage of apoptosis-positive cells in cardiomyocytes after $CoCl_2$ treatment (**Figures 4C to 4H**). In summary, Trim55 knockdown could potentially mitigate hypoxia-induced cardiomyocyte apoptosis.

TRIM55 INDUCED CARDIOMYOCYTE OXIDATIVE STRESS THROUGH THE Nrf2/HO-1 SIGNALING PATHWAY. Numerous studies have shown that excessive production of intracellular ROS can lead to oxidative damage of the cell membrane, which can cause cell apoptosis.[19] Therefore, we hypothesized that Trim55 promoted cardiomyocyte apoptosis through regulating oxidative stress. We first evaluated the effect of Trim55 on oxidative stress in cardiomyocytes. Various well-established antioxidative stress indicators were examined in our study, including P62, Nrf2, and HO-1.[20] After Trim55 overexpression in NRCMs, a significant reduction in the expression levels of P62, Nrf2, and HO-1 proteins was observed (**Figure 5A**). Conversely, the expression levels of P62, Nrf2, and HO-1 were significantly increased after Trim55 knockdown (**Figure 5B**).

The generation and scavenging of ROS are essential for maintaining the redox state within the cell. Oxidative stress occurs when redox reactions are imbalanced.[21] To detect changes in intracellular ROS content, Trim55-overexpressing H9C2 cells were given CellROX staining followed by confocal microscopy photography and flow cytometry analysis. Trim55 overexpression significantly increased intracellular ROS production. However, Trim55 knockdown did not affect intracellular ROS production (**Figures 5C to 5F**).

There is growing evidence that activation of the Nrf2/HO-1 pathway exerts antioxidant effects and protects against myocardial infarct-induced adverse cardiac remodeling.[22,23] Therefore, to further clarify whether the mechanism by which Trim55 promotes oxidative stress is related to the Nrf2/HO-1 pathway, NRCMs were used for rescue experiments. Trim55 overexpression was combined with Nrf2 overexpression, and the expression levels of HO-1 were detected by Western blot. The results showed that overexpression of Nrf2 could reverse the decrease of HO-1 expression induced by Trim55 overexpression (Supplemental Figure 6A). Next, to examine the changes in intracellular ROS content, we overexpressed Trim55 and Nrf2 in H9C2 cells, and CellROX staining was performed by using flow cytometry and confocal microscopy. The results showed that Nrf2 overexpression partially reversed the increase of intracellular ROS induced by Trim55 overexpression (Supplemental Figures 6B to 6D). In contrast, Nrf2 expression was knocked down after low Trim55 expression. Nrf2 knockdown could reduce the increase of HO-1 caused by Trim55 low expression (Supplemental Figure 6E). CellROX staining results showed that Nrf2 knockdown increased the reduction of intracellular ROS induced by Trim55 knockdown (Supplemental Figures 6F to 6H). These results indicate that Trim55 induced oxidative stress in cardiomyocytes through inhibiting the Nrf2/HO-1 pathway.

TRIM55 PROMOTED CARDIOMYOCYTE APOPTOSIS THROUGH INHIBITING THE Nrf2/HO-1 SIGNALING PATHWAY. It is well known that HO-1 is considered as a target of Nrf2. Nrf2/HO-1, as a classical antioxidative stress pathway, plays an important role in cardiomyocyte apoptosis.[24] Therefore, we overexpressed Trim55 and HO-1 in NRCMs and then assessed cell apoptosis by Western blot, flow cytometry, and TUNEL staining. The results showed that overexpression of HO-1 could significantly reverse the increase in the level of apoptotic proteins, the increase in the proportion of apoptosis-positive cells, and the increase in the number of TUNEL-positive cells caused by Trim55 overexpression (**Figures 6A to 6C**). Conversely, low expression of HO-1 aggravated cell apoptosis in Trim55-knockdown cardiomyocytes (**Figures 6D and 6F**). Therefore, considering that Trim55 is an E3 ubiquitin ligase, to further clarify the specific mechanism of Trim55 regulating the Nrf2/HO-1 pathway, we clarified the protein half-life and degradation pathway of Nrf2. The transcription level of Nrf2 remained unchanged following Trim55 overexpression or knockdown (Supplemental Figure 7A), suggesting that Trim55 might regulate the protein degradation of Nrf2. Therefore, the half-life period and protein degradation pathway were

FIGURE 3 **Trim55 Overexpression Promoted Cardiomyocyte Apoptosis Induced by Hypoxia**

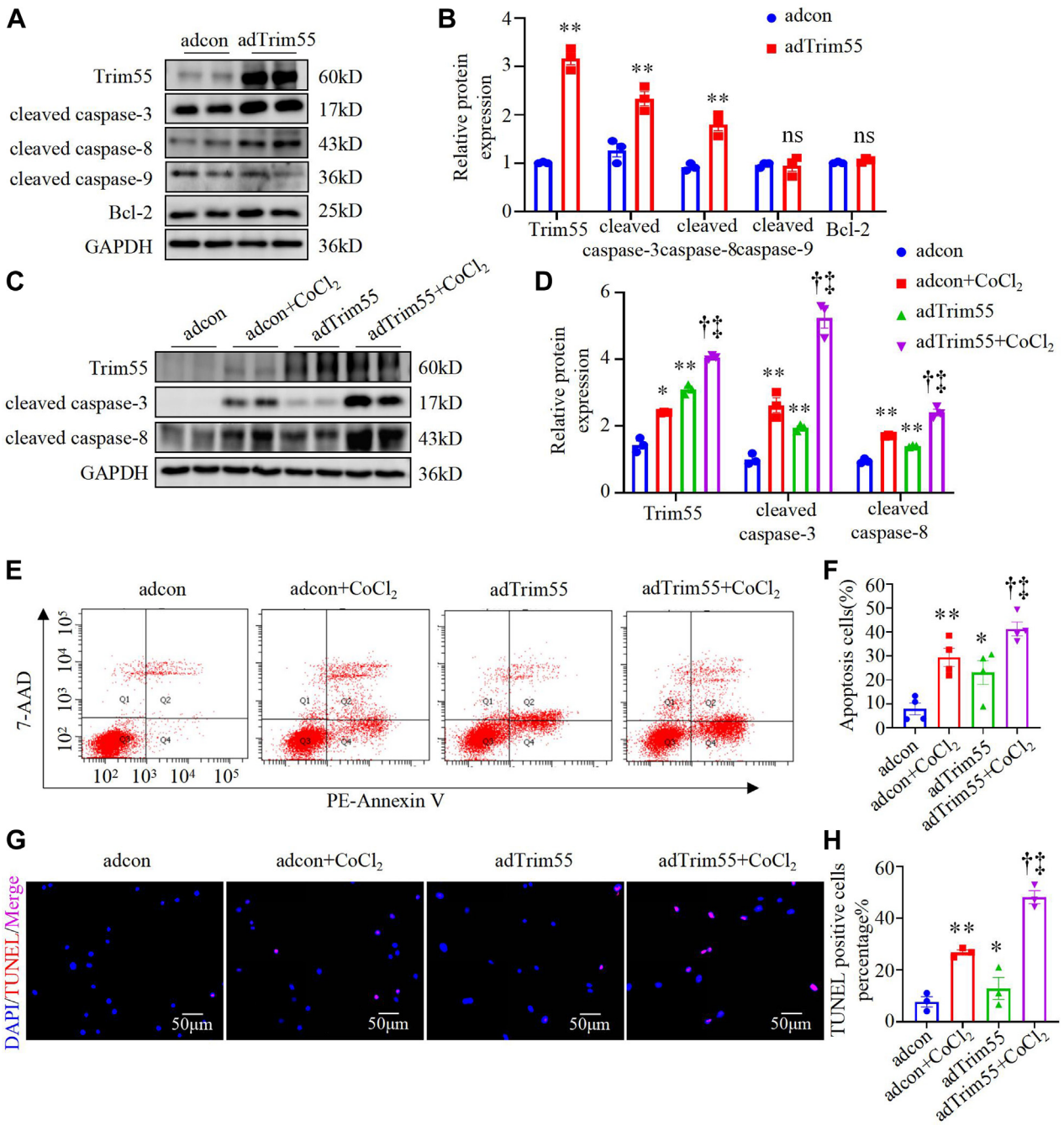

(A, B) Quantification and representative images of Western blots showing the expression of apoptosis-related proteins after Trim55 overexpression (n = 3). (C, D) Effects of Trim55 overexpression and $CoCl_2$ treatment on the expression of apoptosis-related proteins by Western blot (n = 3). (E, F) Effects of Trim55 overexpression and $CoCl_2$ treatment on cardiomyocyte apoptosis by flow cytometry analysis (n = 4). (G, H) Effects of Trim55 overexpression and $CoCl_2$ treatment on cardiomyocyte apoptosis by TUNEL staining (n = 3). $CoCl_2$: 400 μmol/L, 24 hours. All data in B, D, F, and H are expressed as mean ± SEM. Data in B were analyzed using an unpaired Student's *t*-test. Data in D, F, and H were analyzed using 2-way analysis of variance followed by the Bonferroni post hoc test. $^*P < 0.05$, $^{**}P < 0.01$ vs adcon; $^{\dagger}P < 0.05$ vs adTrim55; $^{\ddagger}P < 0.05$ vs adcon + $CoCl_2$. adcon = adenovirus control; adTrim55 = Trim55-overexpressing adenovirus; DAPI = 4′,6-diamidino-2-phenylindole; ns = not significant; other abbreviations as in Figures 1 and 2.

FIGURE 4 Trim55 Knockdown Alleviated Cardiomyocyte Apoptosis Induced by Hypoxia

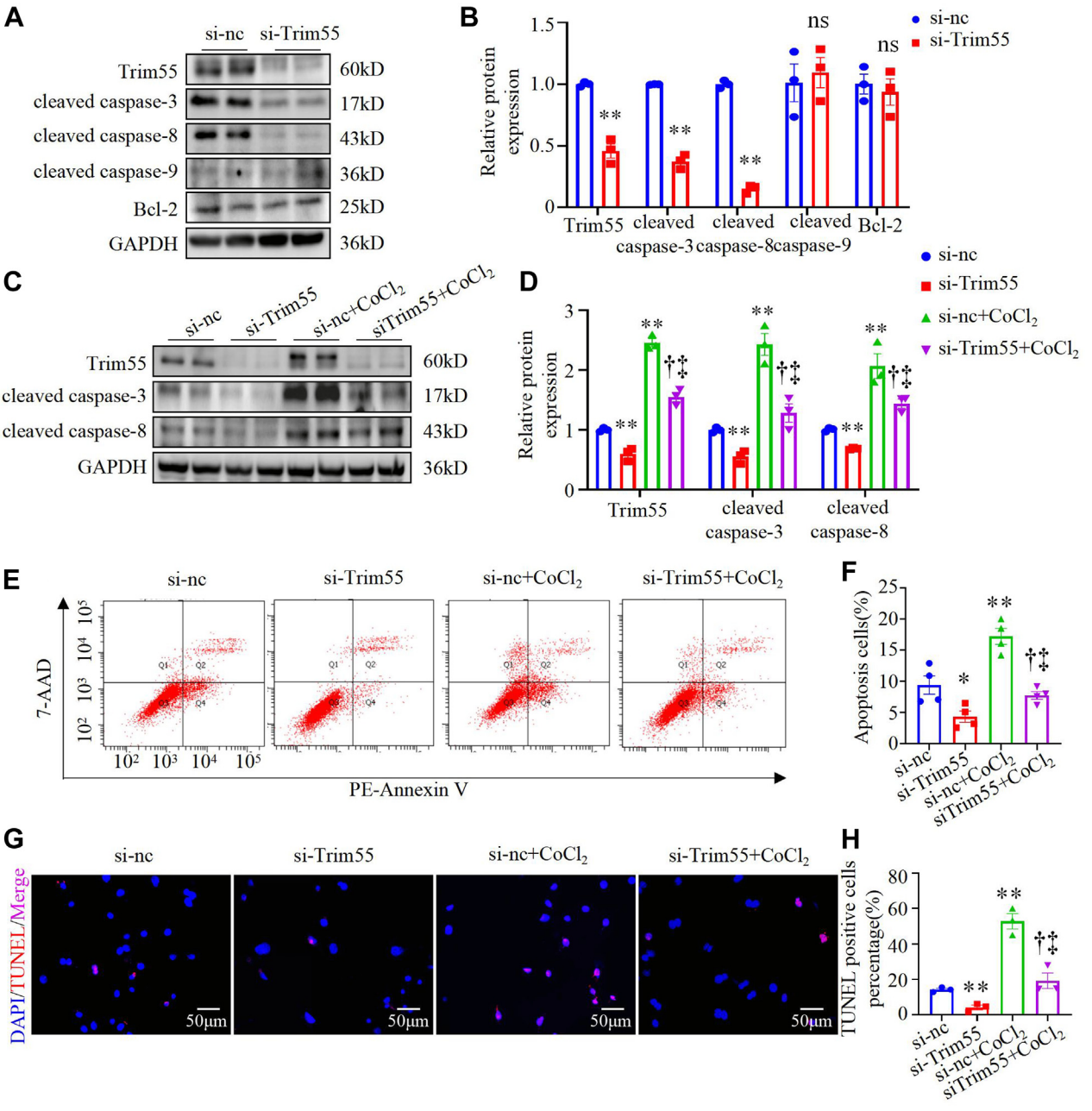

(A, B) Quantification and representative images of Western blot analyses showing the expression of apoptosis-related proteins after Trim55 knockdown (n = 3). (C, D) Effects of Trim55 knockdown and $CoCl_2$ treatment on the expression of apoptosis-related proteins by Western blot (n = 3). (E, F) Effects of Trim55 knockout and $CoCl_2$ treatment on cardiomyocyte apoptosis by flow cytometry analysis (n = 4). (G, H) Effects of Trim55 knockdown and $CoCl_2$ treatment on cardiomyocyte apoptosis by TUNEL staining (n = 3). All data in B, D, F, and H are expressed as mean ± SEM. Data in B were analyzed using an unpaired Student's *t*-test. Data in D, F, and H were analyzed using 2-way analysis of variance, followed by the Bonferroni post hoc test. $^{*}P < 0.05$, $^{**}P < 0.01$ vs si-nc; $^{‡}P < 0.05$ vs si-Trim55; $^{†}P < 0.05$ vs si-nc + $CoCl_2$. si-nc = siRNA-normal control; si-Trim55 = Trim55-interfering RNA; other abbreviations as in Figures 1 to 3.

FIGURE 5 Trim55 Promoted Oxidative Stress by Inhibiting the Nrf2/HO-1 Pathway in Cardiomyocytes

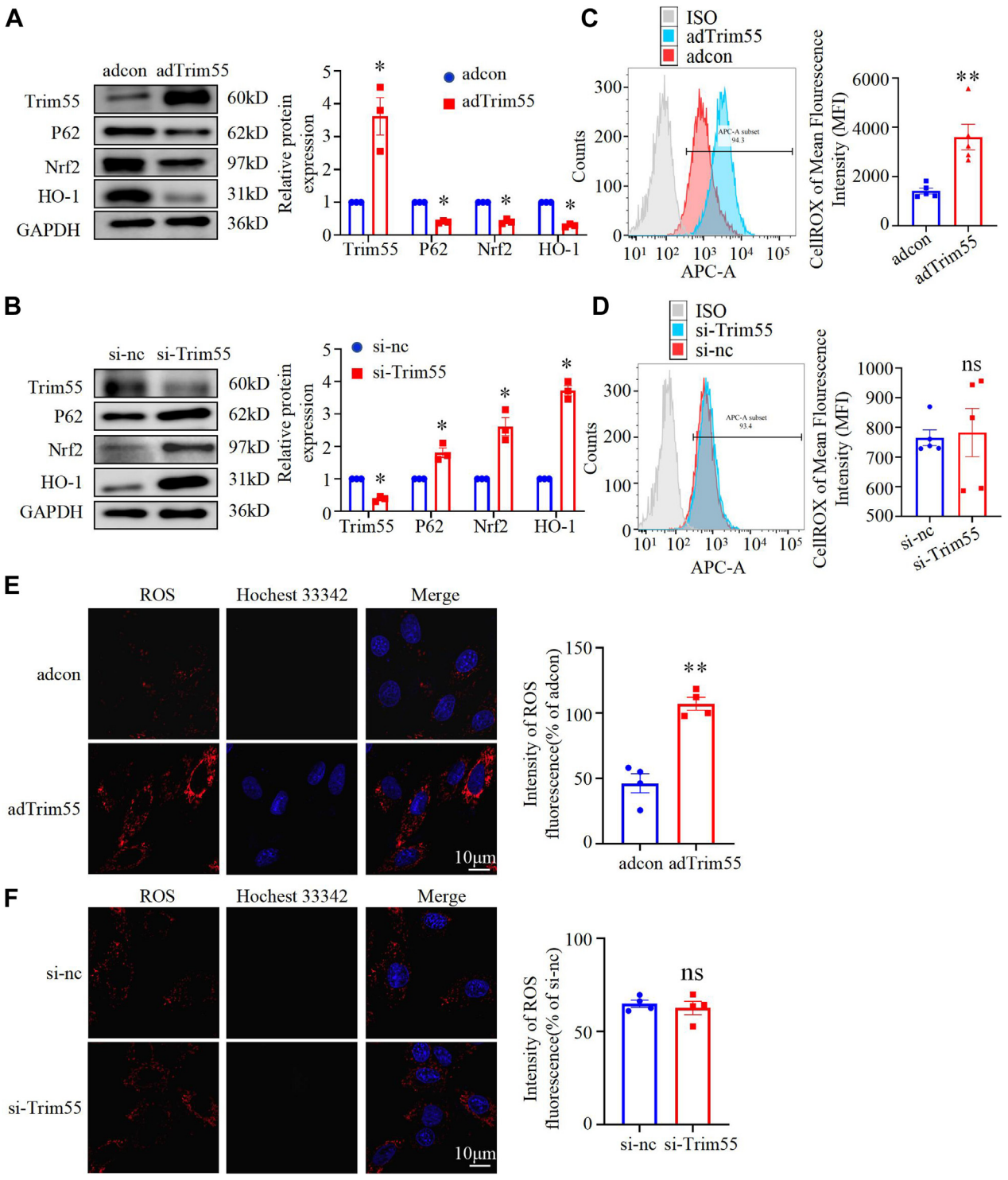

(A) Quantification and representative images of Western blot analyses showing the expression of antioxidant proteins (P62, Nrf2, HO-1) after overexpression of Trim55 in cardiomyocytes (n = 3). (B) Quantification and representative images of Western blot analyses showing the expression of antioxidant proteins (P62, Nrf2, HO-1) after Trim55 knockdown (n = 3). (C) Effects of Trim55 overexpression on the intracellular ROS levels by flow cytometry (n = 5). (D) Effects of Trim55 silencing on the intracellular ROS levels by flow cytometry (n = 5). (E) Quantification and representative images of CellROX staining after Trim55 overexpression (n = 3). (F) Quantification and representative images of CellROX staining after Trim55 knockdown (n = 3). All data in A to F are expressed as mean ±SEM. Data in A to F were analyzed by Student's *t*-test. $*P < 0.05$, $**P < 0.01$ vs adcon or si-nc. APC = allophycocyanin; HO-1 = heme oxygenase 1; ISO = isotype control; Nrf2 = nuclear factor, erythroid derived 2; ROS = reactive oxygen species; other abbreviations as in Figures 1 to 4.

FIGURE 6 Trim55 Promoted Cardiomyocyte Apoptosis Through Inhibiting the Nrf2/HO-1 Signaling Pathway

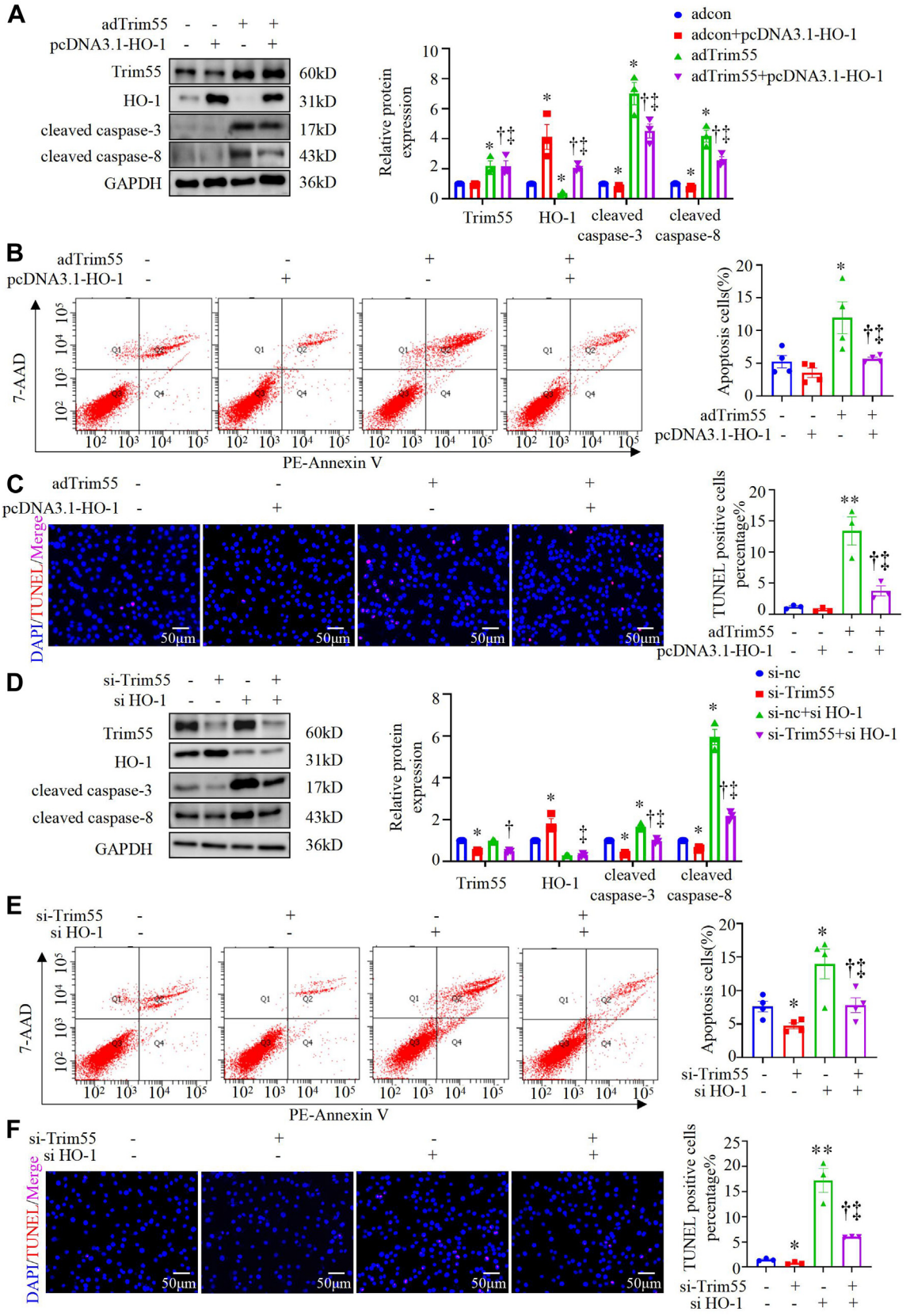

Continued on the next page

analyzed. A steady decrease in the abundance of Nrf2 protein began to decrease at the 3-hour timepoint after CHX treatment (Supplemental Figures 7B and 7C). Following the administration of the proteasome pathway inhibitor (MG132) and CQ (a lysosome inhibitor) into NRCMs, Western blot analysis revealed that the protein degradation of Nrf2 primarily occurred through the proteasome pathway (Supplemental Figures 7B and 7C). To further verify the relationship between Trim55 and Nrf2 degradation, we administered CHX or MG132 in Trim55-overexpressing NRCMs. The results showed that overexpression of Trim55 shortened the half-life of Nrf2 and accelerated its degradation (Supplemental Figures 7D and 7E).

In addition, coimmunoprecipitation showed that there was a protein interaction between Trim55 and Nrf2 (Supplemental Figure 7F). These results suggest that Trim55 accelerated the degradation of Nrf2 by binding to Nrf2 and inhibited the expression of the HO-1 protein, thereby promoting cardiomyocyte apoptosis.

TRIM55 WAS REGULATED BY THE TRANSCRIPTION FACTOR FOXO3 UNDER HYPOXIA. To determine the cause of the increased Trim55 transcript levels after hypoxic injury, several potential transcription factors in the promoter of Trim55 gene were identified by the UCSC database (http://genome.ucsc.edu) and the JASPAR library (http://jaspar.genereg.net).[25,26] Among the transcription factors, only Foxo3 expression showed a substantial increase in cardiomyocytes after hypoxia (**Figures 7A and 7B**). Then, we validated this result in vivo and found that Foxo3 expression was also significantly increased in the border zone after MI (**Figures 7C and 7D**). Furthermore, we assessed the protein and transcriptional levels of Trim55 after Foxo3 overexpression in cardiomyocytes. Foxo3 overexpression significantly increased the protein and transcriptional levels of Trim55 (**Figures 7E to 7G**). Conversely, Foxo3 knockdown resulted in a considerable decrease in the mRNA and protein expression of Trim55 (**Figures 7H to 7J**).

To characterize the relationship between Foxo3 and Trim55, we used the JASPAR library to predict candidate binding sites for the transcription factor Foxo3 in the promoter regions of Trim55[26] (**Figure 7K**). All possible Foxo3 binding sites in the Trim55 promoter region were mutated by constructing a mutant Trim55 promoter plasmid (Mut-Trim55) and the WT Trim55 promoter plasmid (WT-Trim55). The result revealed that Foxo3 overexpression increased the luciferase activity in WT-Trim55 plasmid-transfected HEK293T; however, Foxo3 overexpression did not affect the luciferase activity in Mut-Trim55 plasmid-transfected HEK293T (**Figure 7L**). These results indicate that Foxo3 was a direct upstream transcription factor of Trim55 promoter, which directly increased the transcriptional and protein expression of Trim55 after hypoxia.

DISCUSSION

This study revealed that Trim55, an E3 ubiquitin ligase, plays a critical role in cardiomyocyte apoptosis after MI in vivo and in vitro. The main findings are as follows: 1) The transcriptional and protein levels of Trim55 were up-regulated in the infarcted border zone and hypoxic cardiomyocytes. 2) Trim55 knockout significantly improved cardiac function and alleviated cardiomyocyte apoptosis after MI, whereas Trim55 overexpression aggravated cardiac dysfunction and cardiomyocyte apoptosis after MI. 3) Mechanistically, Trim55 inhibited the Nrf2/HO-1 antioxidant signaling pathway and induced oxidative stress in cardiomyocytes, thereby aggravating cardiomyocyte apoptosis. 4) Foxo3 was a direct upstream transcription factor of the Trim55 gene promoter. These findings reveal that Trim55 is a promising therapeutic target for MI.

Trim55 is a ubiquitin ligase of the E3 class that is significantly expressed in cardiac and skeletal muscle tissues.[7] Previous studies have indicated that Trim55 plays an important role in a variety of cardiovascular diseases, including chronic heart failure, diabetic cardiomyopathy, cardiac hypertrophy, and myocardial ischemia/reperfusion injury. However, the role

FIGURE 6 Continued

(A) Effects of Trim55 overexpression and HO-1 overexpression on the expression of Trim55, HO-1, cleaved caspase-3, and cleaved caspase-8 by Western blot (n = 3). (B) Effects of Trim55 overexpression and HO-1 overexpression on cardiomyocyte apoptosis by flow cytometry (n = 4). (C) Effects of Trim55 overexpression and HO-1 overexpression on cardiomyocyte apoptosis by TUNEL staining (n = 3). (D) Effects of Trim55 knockdown and HO-1 knockdown on the expressions of cleaved caspase-3 and cleaved caspase-8 by Western blot (n = 3). (E) Effects of Trim55 knockdown and HO-1 knockdown on cardiomyocyte apoptosis by flow cytometry (n = 4). (F) Effects of Trim55 knockdown and HO-1 knockdown on cardiomyocyte apoptosis by TUNEL staining (n = 3). All data in A to F are expressed as mean ± SEM. Data in A to F were analyzed by 2-way analysis of variance followed by the Bonferroni post hoc test. *$P < 0.05$, **$P < 0.01$ vs adcon or si-nc; $^{\dagger}P < 0.05$ vs adTrim55 or si-nc + si HO-1; $^{\ddagger}P < 0.05$ vs adcon + pcDNA3.1 HO-1 or si-Trim55. Abbreviations as in **Figures 1 to 5**.

FIGURE 7 Foxo3 Was a Direct Upstream Transcription Factor of Trim55

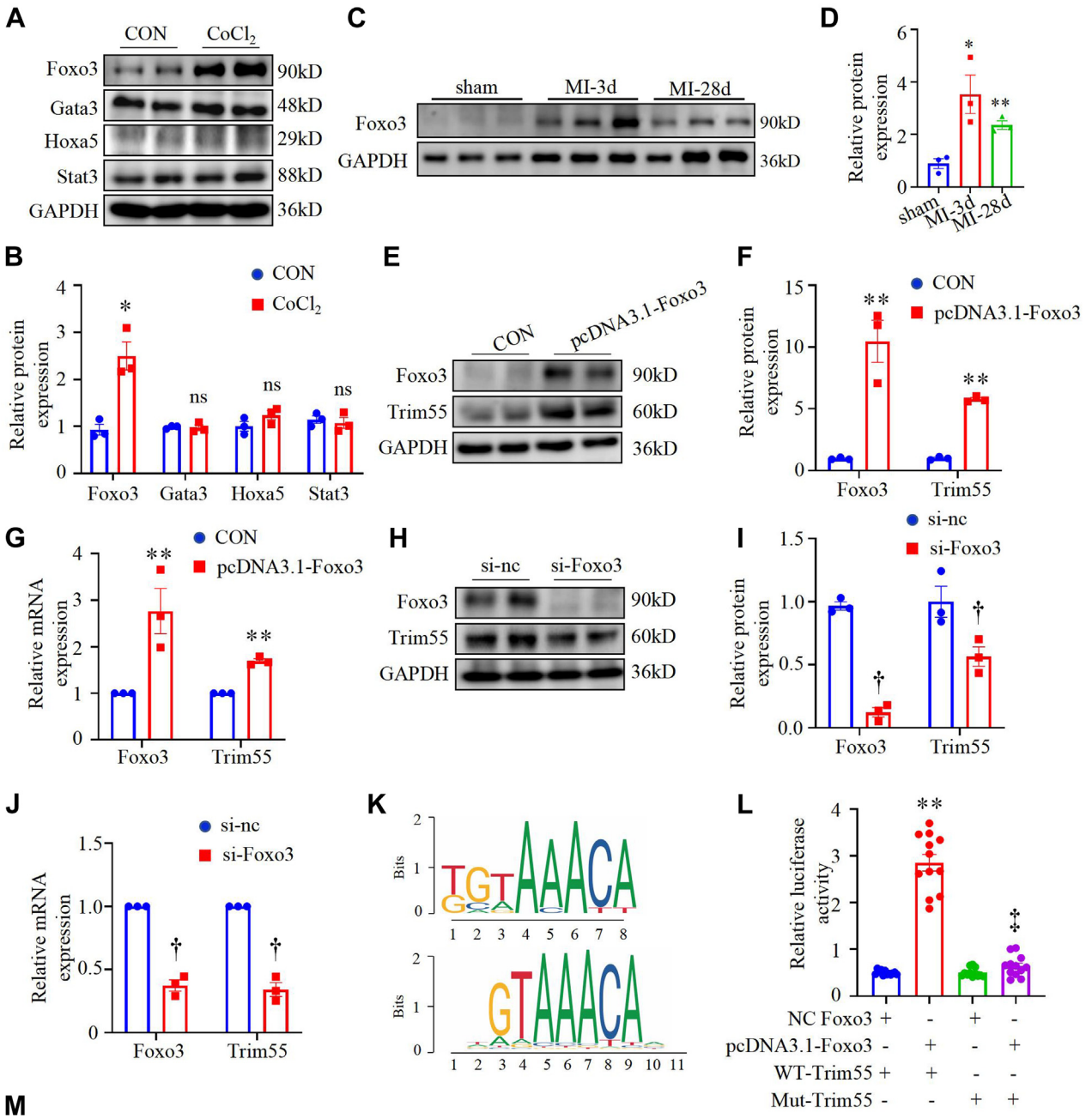

Continued on the next page

and mechanism of Trim55 in regulating myocardial injury after MI has not been fully elucidated. In our study, we found that Trim55 was up-regulated in the border zone after MI. In vitro, Trim55 expression in cardiomyocytes was significantly increased in a time- and concentration-dependent manner after hypoxia. Previous studies have shown that Trim55 is closely related to cardiomyocyte survival. For instance, up-regulation of Trim55 was observed in the cardiac tissue of individuals with chronic heart failure,[27] and overexpression of the Trim55 E140K mutant, achieved through the use of CRISPR/Cas9 technology, resulted in a notable reduction in the survival rate of cardiomyocytes;[28] Trim55 promotes cardiomyocyte apoptosis in myocardial ischemia/reperfusion injury through ubiquitination of dual-specificity phosphatase 1 (DUSP1) and activation of JNK1/2.[12] Our results strongly suggest that Trim55 expression was increased in cardiomyocytes after hypoxic stimuli, which might be related to cardiomyocyte apoptosis. Subsequently, we used gain-of-function and loss-of-function experiments to evaluate the roles of Trim55 on myocardial injury after MI. In vivo, Trim55 knockout significantly improved cardiac function and ameliorated myocardial remodeling after MI, whereas Trim55 overexpression significantly aggravated cardiac dysfunction and myocardial remodeling. However, the mechanism by which Trim55 exerted these effects in MI had not yet been elucidated.

Many studies have shown that a variety of pathogenic factors can participate in the occurrence and development of MI, including inflammation,[29] autophagy,[30] mitochondrial damage,[31] calcium homeostasis,[32,33] extracellular matrix remodeling,[34] oxidative stress,[35,36] and apoptosis.[4,37,38] Studies have shown that cardiomyocyte apoptosis is an important cause of cardiomyocyte death after MI and can promote the progression of heart failure after MI.[4] Our study revealed that Trim55 overexpression aggravated cardiomyocyte apoptosis in the border zone after MI and that Trim55 knockout eliminated cardiomyocyte apoptosis in the border zone after MI in vivo.

In the previous studies, there have been many hypoxia models in vitro, including low oxygen-induced hypoxia (1% O_2) and $CoCl_2$-induced chemical hypoxia. $CoCl_2$ strongly stabilizes HIF1α and HIF2α under normoxic conditions. Compared to 1% O_2-induced hypoxia and the use of other hypoxia mimics, the stabilization of HIF1α and HIF2α is sustained for several hours. Hence, the $CoCl_2$ model allows users a wider time window to manipulate and analyze their samples under normoxic conditions. In addition, $CoCl_2$ produces typical apoptotic changes, cell shrinkage, chromatin condensation, nuclear fragmentation and an extended G2/M phase of the cell cycle, release of cytochrome c, disruption of the mitochondrial transmembrane potential, up-regulation of the voltage-dependent anion channel, and activation of caspases.[1] Therefore, we chose $CoCl_2$ as the hypoxia stimulation in our study. We observed that Trim55 overexpression promoted $CoCl_2$-induced extrinsic apoptosis in cardiomyocytes, including a significant increase in the expression of cleaved caspase-3 and cleaved caspase-8. Caspases act as apical initiators or distal effectors, coordinating apoptotic cell death programs.[39] Two signaling pathways trigger apoptosis using different initiator caspases; however, both converge on the distal effector caspase-3/7.[40] In the endogenous pathway, Bcl-2 is a key regulatory molecule.[41] When Bcl-2 is blocked, more cytochrome c is released, leading to the formation of apoptotic bodies. These apoptotic bodies then control the multimerization of caspase-9 to help it become fully active, cut caspase-3, and turn it on to start apoptosis.[40] In the exogenous pathway, death ligands and receptor complexes combine with adaptor proteins to form the death-inducing signaling complex (DISC). DISC mediates the activation and self-processing of caspase-8, and the released protease enters the cytosol, cleaves, and activates caspase-3, thereby initiating apoptosis.[42] Although different

FIGURE 7 Continued

(A, B) Quantification and representative images of Western blots showing the expression of Foxo3, Gata3, Hoxa5, and Stat3 after $CoCl_2$ hypoxia in NRCMs (n = 3). *P < 0.05 vs CON. (C, D) Foxo3 expression in the myocardium post-MI. (n = 3). *P < 0.05, **P < 0.01 vs sham (E, F) Quantification and representative images of Western blot analyses showing the expression of Trim55 after Foxo3 overexpression in NRCMs (n = 3). **P < 0.01 vs CON. (G) Quantification of Trim55 mRNA levels in NRCMs after Foxo3 overexpression (n = 3). **P < 0.01 vs CON. (H, I) Quantification and representative images of Western blot analyses showing the expression of Trim55 after knockdown in NRCMs (n = 3). $^{\dagger}P$ < 0.05 vs si-nc. (J) Quantification of Trim55 mRNA levels in NRCMs after Foxo3 knockdown (n = 3). $^{\dagger}P$ < 0.05 vs si-nc. (K) Possible binding sites of Foxo3 and Trim55 were predicted using the JASPAR website. (L) Relative luciferase activity in HEK293T cells with cotransfection with Foxo3-overexpressing plasmid and with WT-Trim55 plasmid or Mut-Trim55 plasmid. **P < 0.01 vs NC Foxo3 + WT-Trim55; $^{\ddagger}P$ < 0.05 vs NC Foxo3 + Mut-Trim55 (n = 12). (M) The effect of Trim55 on cardiomyocyte apoptosis after MI (by Figdraw). All data in B, D, F, G, H, and J are expressed as mean ± SEM. Data in B, D, F, G, and H were analyzed using Student's t-test. Data in J were analyzed using 2-way analysis of variance, followed by the Bonferroni post hoc test. Foxo3 = forkhead box transcription factor 3; Mut = mutated; NC = normal control; WT = wild type; other abbreviations as in Figures 1 to 5.

caspases mediate the 2 apoptotic pathways, there is complex crosstalk between the pathways. Therefore, we believe that Trim55 regulated the apoptosis in the border zone after MI mainly by mediating the exogenous apoptosis of cardiomyocytes.

Oxidative stress plays an important role in cardiomyocyte aopoptosis.[14,19,43] The Nrf2/HO-1 pathway plays a protective role in various cell types by inhibiting apoptosis.[44-46] Nrf2 is a transcription factor for HO-1.[47] After MI, HO-1 transgenic mice show significant improvement in cardiac function and a significant reduction in infarct size, indicating that the overexpression of HO-1 reduced oxidative stress and apoptosis, exerting cardioprotective effects.[48] Herein, we observed the effect of Trim55 on the expressions of Nrf2 and HO-1. The results showed that Trim55 overexpression inhibited the protein levels of Nrf2 and HO-1 and that Trim55 knockout elevated the protein levels of Nrf2 and HO-1 in NRCMs. Intracellular ROS content was detected by CellROX staining, and the results showed that Trim55 overexpression significantly increased intracellular ROS content but that Trim55 low expression had no effect on intracellular ROS content. This may be caused by the fact that although the expression of Nrf2 in NRCMs was significantly increased after Trim55 knockdown, it was still in a physiologic state and could not be completely distinguished from normal cells. Furthermore, the up-regulation of Trim55 increased the protein levels of cleaved caspase-3 and cleaved caspase-8 in cardiomyocytes by inhibiting the Nrf2/HO-1 antioxidative stress pathway, thereby aggravating cardiomyocyte apoptosis.

Because Trim55 is an E3 ubiquitin ligase, studies have reported that Trim55 acts as an E3 ubiquitin ligase to ubiquitinate PPARα and PPARγ1 in vivo and regulates diabetic cardiomyopathy,[11] and E3 ubiquitin ligase is a key step in the degradation of proteins by the ubiquitin-proteasome system.[49] In our study, Trim55 could interact with Nrf2 and affect Nrf2 protein degradation in a proteasome-dependent manner. These results reveal that Trim55 might be an E3 ubiquitin ligase to ubiquitinate Nrf2, thereby affecting the Nrf2/HO-1 pathway.

Foxo3 belongs to the forkhead box transcription factor (Foxo) family.[50] Previous studies have shown that Foxo3 aggravates MI by regulating the transcription of multiple genes in hypoxia cardiomyocytes. For example, Foxo3 promotes myocardial injury after MI by targeting autophagy related 7 (ATG7) promoter.[51] Foxo3 promotes cardiomyocyte death by increasing the expression of BCL2 interacting protein 3 (BNIP3) under hypoxia conditions.[52] In our study, Trim55 expression was increased in the myocardial border zone post-MI, which was regulated by a transcription role in MI.

STUDY LIMITATIONS. Although we demonstrated that Trim55 regulated cardiomyocyte apoptosis via the Nrf2/HO-1 pathway in vitro, whether Trim55 plays the same function in vivo or even in the human heart samples remains unclear. In addition, for in vivo experiments, we used systemic Trim55 overexpression of AAVs to evaluate the effect of Trim55 overexpression on myocardial injury after MI. Trim55 cardiomyocyte-specific overexpression AAV or cardiomyocyte-specific transgenic mice should be used in a future study.

CONCLUSIONS

We observed, for the first time to our knowledge, that Trim55 deletion alleviated cardiac remodeling and improved cardiac function after MI and that Trim55 overexpression aggravated cardiac dysfunction and cardiac remodeling. Trim55 promoted cardiomyocyte apoptosis by inhibiting the Nrf2/HO-1 antioxidant signaling pathway (**Figure 7M**). These findings provide new insights into the function of Trim55 in MI and suggest that Trim55 may be a novel target for the prevention and treatment of MI.

ACKNOWLEDGMENTS The authors are grateful to all the participants of this work. All data generated or analyzed during this study are included in the published article.

FUNDING SUPPORT AND AUTHOR DISCLOSURES

This work was supported by the National Natural Science Foundation of China (82070308, 82170297, and 82200431), the China National Key R&D Project (2022YFC2503403, 2020YFC2008100), the Excellent Youth Fund of Liaoning Natural Science Foundation (2021-YQ-03), the Liaoning Science and Technology Project (2022JH2/101300012), and the General project of Joint Fund of Science and Technology Plan of Liaoning Province (2023-MSLH-366). The authors have reported that they have no relationships relevant to the contents of this paper to disclose.

ADDRESS FOR CORRESPONDENCE: Dr Yaling Han, State Key Laboratory of Frigid Zone Cardiovascular Disease, Cardiovascular Research Institute and Department of Cardiology, General Hospital of Northern Theater Command, Wenhua Road 83, 110016 Shenyang, China. E-mail: hanyaling@163.net. OR Dr Dan Liu, State Key Laboratory of Frigid Zone Cardiovascular Disease, Cardiovascular Research Institute and Department of Cardiology, General Hospital of Northern Theater Command, Wenhua Road 83, 110016 Shenyang, China. E-mail: ljmuer@sina.com.

PERSPECTIVES

COMPETENCY IN MEDICAL KNOWLEDGE: Cardiomyocyte apoptosis plays an important role in the pathologic process of MI. In this study, we investigated the role and mechanism of Trim55 in cardiomyocyte apoptosis after MI. Trim55 knockout improves cardiac function and inhibits cardiomyocyte apoptosis after MI, whereas Trim55 overexpression aggravates cardiac dysfunction and cardiomyocyte apoptosis after MI. Trim55 interacts with Nrf2 to accelerate the degradation of Nrf2 and inhibits the expression of HO-1, thereby promoting cardiomyocyte apoptosis and aggravating myocardial injury after MI.

TRANSLATIONAL OUTLOOK: The current study identifies Trim55 as a potential therapeutic target for cardiomyocyte apoptosis after MI. Trim55 aggravates oxidative stress and cardiomyocyte apoptosis by inhibiting the Nrf2/HO-1 pathway. Future studies are needed to determine the potential therapeutic benefits of Trim55, particularly by ameliorating the role of cardiomyocyte apoptosis, to prevent and treat heart failure in patients with MI.

REFERENCES

1. Tsao CW, Aday AW, Almarzooq ZI, et al. Heart disease and stroke statistics—2023 update: a report from the American Heart Association. *Circulation*. 2023;147:e93–e621.

2. Li P, Chen J, Li N, You X, Shen L, Zhou N. Real-world major adverse cardiovascular events of nicorandil and nitrate in coronary heart disease in central China: a retrospective cohort study. *Cardiol Discov*. 2023;3:152–158.

3. Mei L, Chen Y, Chen P, et al. Fibroblast growth factor 7 alleviates myocardial infarction by improving oxidative stress via PI3Kalpha/AKT-mediated regulation of Nrf2 and HXK2. *Redox Biol*. 2022;56:102468.

4. Del Re DP, Amgalan D, Linkermann A, Liu Q, Kitsis RN. Fundamental mechanisms of regulated cell death and implications for heart disease. *Physiol Rev*. 2019;99:1765–1817.

5. Perera S, Mankoo B, Gautel M. Developmental regulation of MURF E3 ubiquitin ligases in skeletal muscle. *J Muscle Res Cell Motil*. 2012;33:107–122.

6. Lange S, Xiang F, Yakovenko A, et al. The kinase domain of titin controls muscle gene expression and protein turnover. *Science*. 2005;308:1599–1603.

7. Bian H, Gao S, Zhang D, et al. The E3 ubiquitin ligase MuRF2 attenuates LPS-induced macrophage activation by inhibiting production of inflammatory cytokines and migration. *FEBS Open Bio*. 2018;8:234–243.

8. Li X, Huang L, Gao W. Overexpression of tripartite motif containing 55 (TRIM55) inhibits migration and invasion of hepatocellular carcinoma (HCC) cells via epithelial-mesenchymal transition and matrix metalloproteinase-2 (MMP2). *Med Sci Monit*. 2019;25:771–777.

9. Prestes PR, Marques FZ, Lopez-Campos G, et al. Tripartite motif-containing 55 identified as functional candidate for spontaneous cardiac hypertrophy in the rat locus cardiac mass 22. *J Hypertens*. 2016;34:950–958.

10. Su M, Wang J, Kang L, et al. Rare variants in genes encoding MuRF1 and MuRF2 are modifiers of hypertrophic cardiomyopathy. *Int J Mol Sci*. 2014;15:9302–9313.

11. He J, Quintana MT, Sullivan J, et al. MuRF2 regulates PPARgamma1 activity to protect against diabetic cardiomyopathy and enhance weight gain induced by a high fat diet. *Cardiovasc Diabetol*. 2015;14:97.

12. Tan J, Shen J, Zhu H, et al. miR-378a-3p inhibits ischemia/reperfusion-induced apoptosis in H9C2 cardiomyocytes by targeting TRIM55 via the DUSP1-JNK1/2 signaling pathway. *Aging (Albany NY)*. 2020;12:8939–8952.

13. Strom J, Chen QM. Loss of Nrf2 promotes rapid progression to heart failure following myocardial infarction. *Toxicol Appl Pharmacol*. 2017;327:52–58.

14. Chu SY, Peng F, Wang J, et al. Catestatin in defense of oxidative-stress-induced apoptosis: A novel mechanism by activating the beta2 adrenergic receptor and PKB/Akt pathway in ischemic-reperfused myocardium. *Peptides*. 2020;123:170200.

15. Ahn HY, Fairfull-Smith KE, Morrow BJ, et al. Two-photon fluorescence microscopy imaging of cellular oxidative stress using profluorescent nitroxides. *J Am Chem Soc*. 2012;134:4721–4730.

16. Kim D, Min D, Kim J, et al. Nutlin-3a induces KRAS mutant/p53 wild type lung cancer specific methuosis-like cell death that is dependent on GFPT2. *J Exp Clin Cancer Res*. 2023;42:338.

17. Lima BHM, Cartarozzi LP, Kyrylenko S, Ferreira RS Jr, Barraviera B, Oliveira ALR. Embryonic stem cells overexpressing high molecular weight FGF2 isoform enhance recovery of preganglionic spinal root lesion in combination with fibrin biopolymer mediated root repair. *Stem Cell Res Ther*. 2024;15:63.

18. Munoz-Sanchez J, Chanez-Cardenas ME. The use of cobalt chloride as a chemical hypoxia model. *J Appl Toxicol*. 2019;39:556–570.

19. Hu N, Sun M, Lv N, et al. ROS-suppression nanoplatform combined activation of STAT3/Bcl-2 pathway for preventing myocardial infarction in mice. *ACS Appl Mater Interfaces*. 2024;16(10):12188–12201.

20. Carroll B, Otten EG, Manni D, et al. Oxidation of SQSTM1/p62 mediates the link between redox state and protein homeostasis. *Nat Commun*. 2018;9:256.

21. Lennicke C, Cocheme HM. Redox metabolism: ROS as specific molecular regulators of cell signaling and function. *Mol Cell*. 2021;81:3691–3707.

22. Shi J, Hou J, Sun Y, et al. Chaihujialonggumulitang shows psycho-cardiology therapeutic effect on acute myocardial infarction with comorbid anxiety by the activation of Nrf2/HO-1 pathway and suppression of oxidative stress and apoptosis. *Biomed Pharmacother*. 2022;153:113437.

23. Elasoru SE, Rhana P, de Oliveira Barreto T, et al. Andrographolide protects against isoproterenol-induced myocardial infarction in rats through inhibition of L-type Ca(2+) and increase of cardiac transient outward K(+) currents. *Eur J Pharmacol*. 2021;906:174194.

24. Yang X, Fang Y, Hou J, et al. The heart as a target for deltamethrin toxicity: inhibition of Nrf2/HO-1 pathway induces oxidative stress and results in inflammation and apoptosis. *Chemosphere*. 2022;300:134479.

25. Lee CM, Barber GP, Casper J, et al. UCSC Genome Browser enters 20th year. *Nucleic Acids Res*. 2020;48:D756–D761.

26. Castro-Mondragon JA, Riudavets-Puig R, Rauluseviciute I, et al. JASPAR 2022: the 9th release of the open-access database of transcription factor binding profiles. *Nucleic Acids Res*. 2022;50:D165–D173.

27. Adams V, Bowen TS, Werner S, et al. Small-molecule-mediated chemical knock-down of MuRF1/MuRF2 and attenuation of diaphragm

dysfunction in chronic heart failure. *J Cachexia Sarcopenia Muscle*. 2019;10:1102–1115.

28. Heliste J, Chheda H, Paatero I, et al. Genetic and functional implications of an exonic TRIM55 variant in heart failure. *J Mol Cell Cardiol*. 2020;138:222–233.

29. Horckmans M, Bianchini M, Santovito D, et al. Pericardial adipose tissue regulates granulopoiesis, fibrosis, and cardiac function after myocardial infarction. *Circulation*. 2018;137:948–960.

30. Popov SV, Mukhomedzyanov AV, Voronkov NS, et al. Regulation of autophagy of the heart in ischemia and reperfusion. *Apoptosis*. 2023;28:55–80.

31. Chen K, He L, Li Y, et al. Inhibition of GPR35 preserves mitochondrial function after myocardial infarction by targeting calpain 1/2. *J Cardiovasc Pharmacol*. 2020;75:556–563.

32. McCarroll CS, He W, Foote K, et al. Runx1 deficiency protects against adverse cardiac remodeling after myocardial infarction. *Circulation*. 2018;137:57–70.

33. Jiao L, Li M, Shao Y, et al. lncRNA-ZFAS1 induces mitochondria-mediated apoptosis by causing cytosolic Ca(2+) overload in myocardial infarction mice model. *Cell Death Dis*. 2019;10:942.

34. He Q, Wang F, Honda T, James J, Li J, Redington A. Loss of miR-144 signaling interrupts extracellular matrix remodeling after myocardial infarction leading to worsened cardiac function. *Sci Rep*. 2018;8:16886.

35. Cadenas S. ROS and redox signaling in myocardial ischemia-reperfusion injury and cardioprotection. *Free Radic Biol Med*. 2018;117:76–89.

36. Yang Z, Wu QQ, Xiao Y, et al. Aucubin protects against myocardial infarction-induced cardiac remodeling via nNOS/NO-regulated oxidative stress. *Oxid Med Cell Longev*. 2018;2018:4327901.

37. Qi B, Song L, Hu L, et al. Cardiac-specific overexpression of Ndufs1 ameliorates cardiac dysfunction after myocardial infarction by alleviating mitochondrial dysfunction and apoptosis. *Exp Mol Med*. 2022;54:946–960.

38. Teringova E, Tousek P. Apoptosis in ischemic heart disease. *J Transl Med*. 2017;15:87.

39. Kesavardhana S, Malireddi RKS, Kanneganti TD. Caspases in cell death, inflammation, and pyroptosis. *Annu Rev Immunol*. 2020;38:567–595.

40. Riedl SJ, Salvesen GS. The apoptosome: signalling platform of cell death. *Nat Rev Mol Cell Biol*. 2007;8:405–413.

41. Chong SJF, Marchi S, Petroni G, Kroemer G, Galluzzi L, Pervaiz S. Noncanonical cell fate regulation by Bcl-2 proteins. *Trends Cell Biol*. 2020;30:537–555.

42. Jin Z, Li Y, Pitti R, et al. Cullin3-based polyubiquitination and p62-dependent aggregation of caspase-8 mediate extrinsic apoptosis signaling. *Cell*. 2009;137:721–735.

43. Duan J, Yin Y, Wei G, et al. Chikusetsu saponin IVa confers cardioprotection via SIRT1/ERK1/2 and Homer1a pathway. *Sci Rep*. 2015;5:18123.

44. Ryter SW. Heme oxgenase-1, a cardinal modulator of regulated cell death and inflammation. *Cells*. 2021;10(3):515.

45. Morse D, Lin L, Choi AM, Ryter SW. Heme oxygenase-1, a critical arbitrator of cell death pathways in lung injury and disease. *Free Radic Biol Med*. 2009;47:1–12.

46. Gozzelino R, Jeney V, Soares MP. Mechanisms of cell protection by heme oxygenase-1. *Annu Rev Pharmacol Toxicol*. 2010;50:323–354.

47. Choi JW, Jo SW, Kim DE, Paik IY, Balakrishnan R. Aerobic exercise attenuates LPS-induced cognitive dysfunction by reducing oxidative stress, glial activation, and neuroinflammation. *Redox Biol*. 2024;71:103101.

48. Shan H, Li T, Zhang L, et al. Heme oxygenase-1 prevents heart against myocardial infarction by attenuating ischemic injury-induced cardiomyocytes senescence. *EBioMedicine*. 2019;39:59–68.

49. Asmamaw MD, Liu Y, Zheng YC, Shi XJ, Liu HM. Skp2 in the ubiquitin-proteasome system: a comprehensive review. *Med Res Rev*. 2020;40:1920–1949.

50. Rodriguez-Colman MJ, Dansen TB, Burgering BMT. FOXO transcription factors as mediators of stress adaptation. *Nat Rev Mol Cell Biol*. 2024;25:46–64.

51. Li F, Long TY, Bi SS, Sheikh SA, Zhang CL. circPAN3 exerts a profibrotic role via sponging miR-221 through FoxO3/ATG7-activated autophagy in a rat model of myocardial infarction. *Life Sci*. 2020;257:118015.

52. Chen YF, Pandey S, Day CH, et al. Synergistic effect of HIF-1alpha and FoxO3a trigger cardiomyocyte apoptosis under hyperglycemic ischemia condition. *J Cell Physiol*. 2018;233:3660–3671.

KEY WORDS apoptosis, HO-1, myocardial infarction, Nrf2, Trim55

APPENDIX For supplemental tables and figures, please see the online version of this paper.